JOURNAL OF MATERIALS SCIENCE 24 (1989) 3289–3294

Study of fatigue crack growth retardation due to overloads in polymethylmethacrylate

Y. IMAI, T. TAKASE, K. NAKANO
Department of Mechanical Engineering, Nagasaki University, Nagasaki, 852, Japan

Retardation of the fatigue crack growth after overloading was investigated in conjunction with the craze deformation at the fatigue crack tip in polymethylmethacrylate. The craze deformation was measured by optical interference and analysed numerically with reference to a previously proposed craze model. In the base line loading, the craze stress concentrates at the crack tip with the applied load and, hence, the non-uniform stress distribution is attained at the maximum load. The overload alters this stress distribution. Just after overloading, the crack tip stress does not reach the previous level, even at the same maximum load. The reduced crack tip stress correlates well with the retarded duration after the overload. It is concluded, therefore, that the craze stress reduction at the crack tip is the cause of crack growth retardation.

1. Introduction

As the region of plastic deformation in some polymers is often confined to a craze zone and is observed microscopically, the stress state around the craze has been of great interest. Following Knight's calculation [1] for an isolated craze, many craze models [2] have been proposed. Recently, perceiving the deformation of craze at the crack tip, Williams [3], and Döll *et al.* [4] attempted to study the mechanism of fatigue crack growth using the Dugdale model and quantitative investigations have been made assuming the uniform stress distribution along the craze. Lauterwasser and Kramer [5], on the other hand, using the density measurement of crazes on thin polystylene films, calculated the craze displacement and stresses. This method, however, may not be applicable to fatigue cracks and crazes in bulk materials. The optical interference method [6, 7], which, although available only for transparent materials, is suitable to use for observing crazes in bulks despite the necessity to assume permanent strain of the craze fibril beforehand.

In this paper, which is based on the modified Dugdale model proposed previously [8], allowing the craze stress to vary along the craze boundary, the method of analysing craze displacement and stress along the craze will be developed at the tip of growing fatigue crack. Crack growth retardation after overload [9] in polymethylmethacrylate (PMMA) will be investigated in association with the alteration of craze stress distribution before and after the overload.

2. Experimental and analysing procedure

2.1. Craze contour measurement

In order to measure optical interference fringes from the crack and craze during the fatigue loading, a special loading device consisting of cam and lever system, shown in Fig. 1, was installed on the microscope stage. Compact-tension specimens, as shown in Fig. 2, were used. The size of the specimen was restricted by the working distance of the objective lens. A fatigue pre-crack was at first introduced from the Chevron notch for each specimen and the measurement of craze geometry was made after the steady state crack growth was attained. The very slow cyclic rate, 1 cycle per minute, was used through the fatigue test in order to follow the geometric change of craze successively during a cycle.

The overload was applied by moving the cam position manually on the loading apparatus. In the course of base-line fatigue loading, we stopped the cam at the minimum load level and changed its position by turning the fixing thread. This procedure took less than 3 sec so that the influence might be small compared to 60 sec for a single complete cycle. Relation between load level and cam position along the lever was calibrated beforehand. After overload, the cam was returned to its previous position and the fatigue loading was continued.

The usual optical interference method was employed to measure the craze contour. Interference patterns from the craze were photographed at several loading levels as well as at maximum and minimum loads in one cycle. For the overload experiment, three successive cycles including before and after overloading were considered. The fringe patterns were traced by a microdensitometer and fringe orders were measured as a function of the distance from the craze tip, r. The increment of craze displacement for one fringe order corresponds to $\lambda/4\mu$, where λ is the wavelength ($\lambda = 546\,\text{nm}$) and μ is the refractive index of craze. The latter was obtained from the following relation with bulk refractive index $\mu_0 = 1.49$ and craze strain ε

$$\frac{\mu^2 - 1}{\mu^2 + 2} = \frac{\mu_0^2 - 1}{\mu_0^2 + 2} \frac{1}{1 + \varepsilon} \tag{1}$$

0022–2461/89 $03.00 + .12

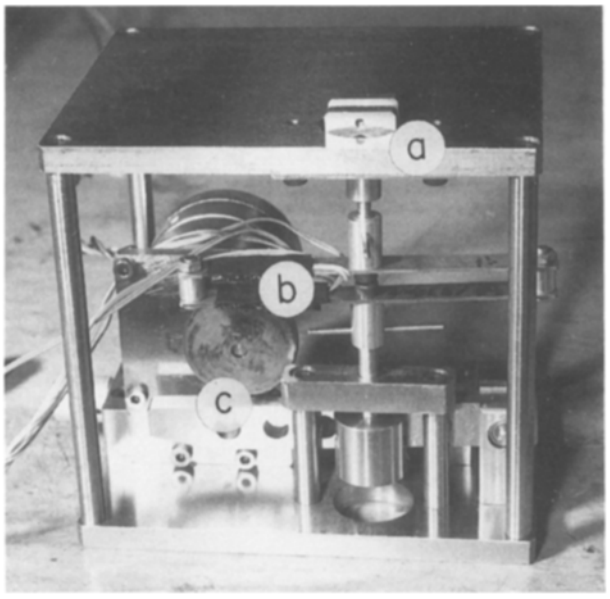

Figure 1 Loading apparatus; a, specimen grip, b, load cell, c, cam and lever.

2.2. Craze stress formulation

The plastically deformed region is confined to a thin craze zone at the tip of a crack. Therefore, the stress state around the crack tip may be well expressed by the Dugdale model, which assumes the plastic zone to be a line.

We consider, here, the elastic stress field around the tip of semi-infinite crack subjected to remote loads corresponding to the stress intensity K_I, as illustrated in Fig. 3. Assuming that the bulk material, the size of which was originally $g(r)$ at a distance r from the craze tip, has deformed, due to the craze stress $\sigma(r)$, into craze fibrils to $\delta(r)$, which is now the size of craze thickness. Note that the Dugdale model gives the elastic displacement of the bulk around the craze zone and also that the elastic displacement of the craze-bulk boundary is $\delta(r) - g(r)$ because the point concerned originally a distance $g(r)$ from the centre line.

With the craze length R, the above may be formulated, with reference to Fig. 3b, as follows

$$\delta(r) - g(r) = \frac{2(1 - \nu^2)}{\pi E} \times \left((2\pi r)^{1/2} K_I - \int_0^R \sigma(s) \log \left| \frac{\sqrt{s} + \sqrt{r}}{\sqrt{s} - \sqrt{r}} \right| \mathrm{d}s \right) \quad (2)$$

and

$$K_I = \left(\frac{2}{\pi} \right)^{1/2} \int_0^R \frac{\sigma(s)}{\sqrt{s}} \mathrm{d}s \quad (3)$$

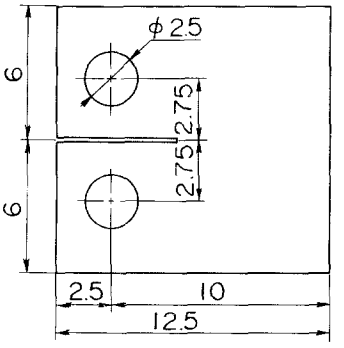

Figure 2 Specimen geometry.

then

$$\delta(r) - g(r) = \frac{2(1 - \nu^2)}{\pi E} \times \int_0^R \sigma(s) \left(2 \left(\frac{r}{s} \right)^{1/2} - \log \left| \frac{\sqrt{s} + \sqrt{r}}{\sqrt{s} - \sqrt{r}} \right| \right) \mathrm{d}s \quad (2)'$$

where E and ν are Young's modulus and Poisson's ratio of the bulk material, respectively, and $E = 3\,\mathrm{GPa}$, $\nu = 0.3$ were used.

We consider, next, the deformation of craze fibrils in Fig. 3a. As long as the crack growth per cycle is much less than the craze length, the craze fibrils near the crack tip can not be produced at one loading cycle but must exist already and have been subjected to many fatigue cycles. Kambour and Kopp [10] have shown that under similar conditions, polycarbonate (PC) craze fibrils tend to deform elastically. The same may hold in this case. The fatigue craze fibrils of PMMA are, then, assumed to deform elastically according to the following relation between the craze stress σ and the total strain ε

$$\varepsilon = e + \sigma/F \quad (4)$$

where e is the permanent strain encountered once at the fibrillation and F the elastic modulus of the matured craze fibril. Then the craze displacement $\delta(r)$ is expressed as

$$\delta(r) = g(r)(1 + e + \sigma(r)/F) \quad (5)$$

$e = 0.5$, $F = 100\,\mathrm{MPa}$ were used in the calculation.

2.3. Method of numerical calculation

Eliminating $g(r)$ from Equations 2′ and 5, we obtain the integral equation of $\sigma(r)$ and $\delta(r)$, which, being combined with Equation 3, may be solved numerically. At first, craze length R is divided into N segments and craze stress $\sigma(r)$ is assumed to vary linearly over

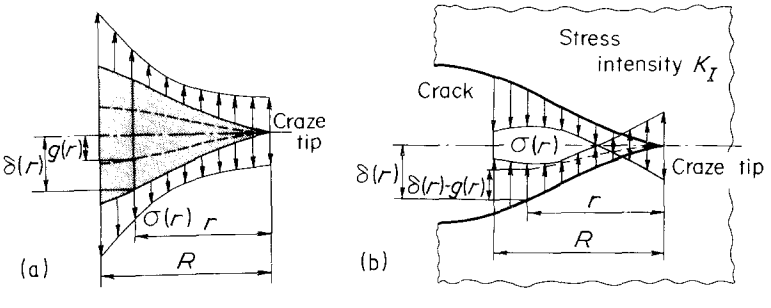

Figure 3 Model of the craze at the tip of semi-infinite crack (a) craze matter, (b) bulk material around the craze.

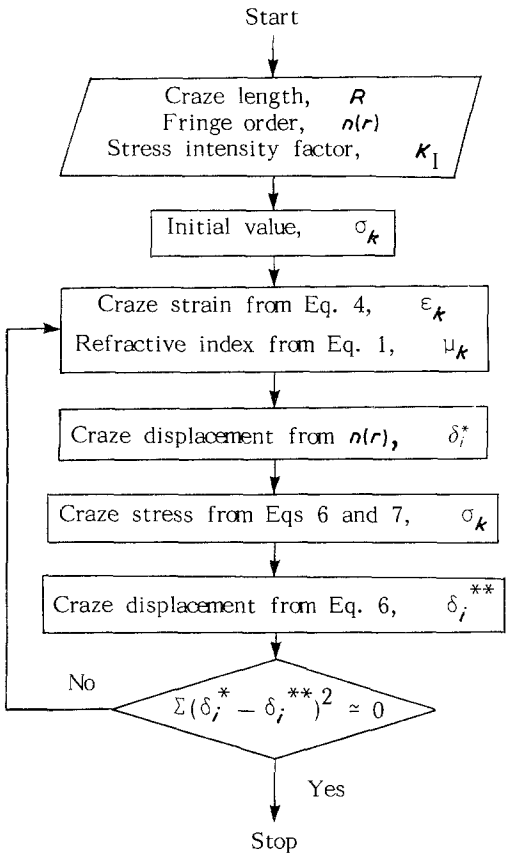

Figure 4 Flow-chart for the iterative calculation of craze stress and displacement.

each segment. That is

$$\sigma(r) = \sigma_{k-1} + (\sigma_k - \sigma_{k-1}) \frac{r - r_{k-1}}{r_k - r_{k-1}}$$
$$(r_{k-1} \leqslant r \leqslant r_k, \quad k = 1, 2, \ldots N)$$

Then, the integral equations are converted into following algebraic equations

$$\sum_{k=1}^{N} (A_k \sigma_{k-1} + B_k \sigma_k) = \frac{\pi E}{2(1 - \nu^2)} \times \frac{\sigma_i + Fe}{\sigma_i + F(1 + e)} \delta(r_i) \quad (6)$$

$$\sum_{k=1}^{N} (C_k \sigma_{k-1} + D_k \sigma_k) = \left(\frac{\pi}{2}\right)^{1/2} K_I \quad (7)$$

where

$$A_k = \int_{r_{k-1}}^{r_k} \left(1 - \frac{s - r_{k-1}}{r_k - r_{k-1}}\right) \times \left[2\left(\frac{r_i}{s}\right)^{1/2} - \log\left|\frac{\sqrt{s} + \sqrt{r_i}}{\sqrt{s} - \sqrt{r_i}}\right|\right] ds$$

$$B_k = \int_{r_{k-1}}^{r_k} \frac{s - r_{k-1}}{r_k - r_{k-1}} \times \left[2\left(\frac{r_i}{s}\right)^{1/2} - \log\left|\frac{\sqrt{s} + \sqrt{r_i}}{\sqrt{s} - \sqrt{r_i}}\right|\right] ds$$

$$C_k = \int_{r_{k-1}}^{r_k} \left(1 - \frac{s - r_{k-1}}{r_k - r_{k-1}}\right) \frac{1}{\sqrt{s}} ds$$

$$D_k = \int_{r_{k-1}}^{r_k} \frac{s - r_{k-1}}{r_k - r_{k-1}} \frac{1}{\sqrt{s}} ds$$

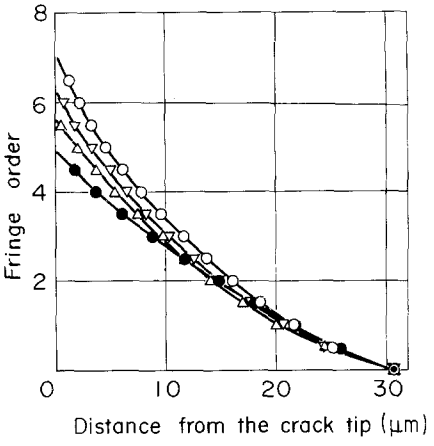

Figure 5 Interference fringe variation during one cycle (● K_I = 0.08 MPa m$^{1/2}$ (min), △ K_I = 0.42 MPa m$^{1/2}$ (loading), ○ K_I = 0.60 MPa m$^{1/2}$ (max) and ▽ K_I = 0.42 MPa m$^{1/2}$ (unloading)).

In the calculation, we used $N = 10$ and set up Equation 6 to 20 terms, (r_i, $i = 1, \ldots, 20$), where the craze displacements, $\delta(r_i)$, were interpolated from the measured. Since the number of equations exceeded the number of unknowns, the least square method was employed to obtain σ_k ($k = 0, 1, \ldots, N$).

Equation 6 involves the unknown σ_i on the right-hand side and, moreover, craze displacement $\delta(r_i)$ should be converted from the measured fringe order by using the refractive index μ, which is to be calculated from Equations 1 and 4. Once more, μ is the function of craze strain. In order to attain consistency, therefore, the calculation was executed iteratively. The flow-chart of the procedure used is shown in Fig. 4.

3. Results and discussion

3.1. Craze stress variation during a fatigue cycle

Photographs were obtained of the craze during loading and unloading for a number of levels of K_I. A typical set of results is shown in Fig. 5. $K_{I_{max}}$, 0.60 MPa m$^{1/2}$, corresponds to the crack growth rate of 0.15 μm cycle^{-1}. The variation near the crack tip is significant in contrast to the one near the craze tip. Even at the $K_{I_{min}}$ level, the crack tip remains open, showing a fringe order of about 5. At loading and unloading periods, dissimilar craze contours were observed even at the same K_I level.

In Fig. 6 these fringe orders were converted into

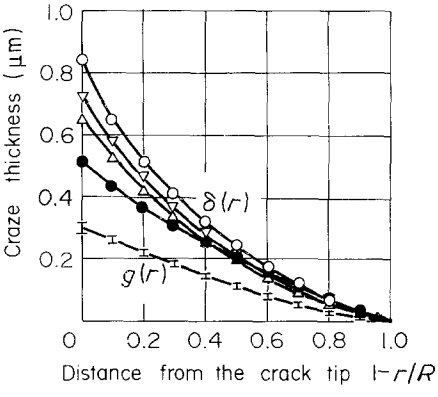

Figure 6 Craze displacement variation during one cycle and the craze original thickness (symbols as for Fig. 5) R = 31 μm.

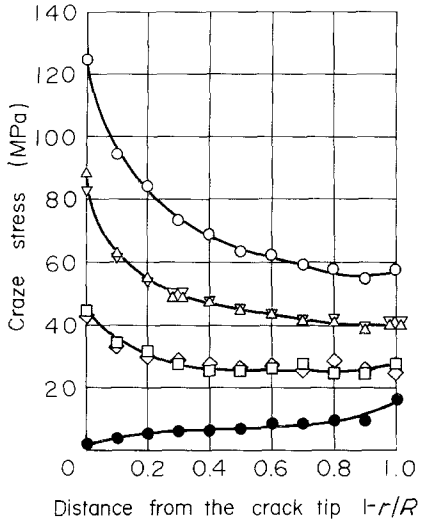

Figure 7 Craze stress variation during one cycle (symbols as for Fig. 5, □ K_I = 0.25 MPa m$^{1/2}$ (loading), ◇ K_I = 0.25 MPa m$^{1/2}$ (unloading)).

displacement. The original craze thickness $g(r)$ is also calculated and shown in the same figure. At the crack tip, the bulk material, originally 0.3 μm thick, deformed into crazes and extended to about 0.8 μm at $K_{I_{max}}$.

The craze stresses $\sigma(r)$, which cause the craze extension, are shown in Fig. 7. Similar stress profiles have been obtained by using other methods [11, 12]. The variation of stress at the crack tip is greatest along the craze, exhibiting very high stress at $K_{I_{max}}$. This high craze stress may bring fibril breakage there resulting in crack growth.

At a level of K_I of about 0.08 MPa m$^{1/2}$, the craze stress at the crack tip reduces to almost zero. A further decrease of K_I induced compression on some part of the craze length. When the crack surfaces become attached and also bear compression stress the craze stress may be somewhat reduced.

3.2. Effect of overload

When an overload is applied in the course of a fatigue cycle, subsequent crack growth usually exhibits retardation as seen in Fig. 8. In this example, a base line load was $K_{I_{max}}$ = 0.61 MPa m$^{1/2}$ and an overload, K_{IOL} = 0.72 MPa m$^{1/2}$, that is, about 18% overload. After a little growth during the overloading, the fatigue crack stopped growing for about a 60 cycle duration.

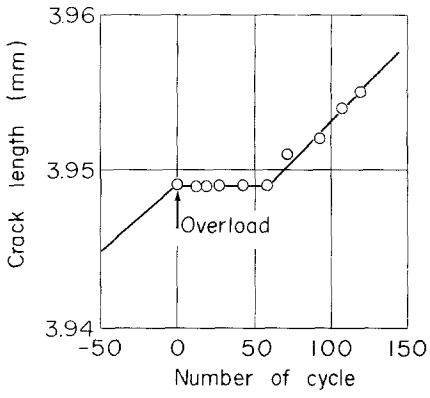

Figure 8 Crack growth retardation due to overloading. K_I = 0.03 to 0.61 MPa m$^{1/2}$, K_{IOL} = 0.72 MPa m$^{1/2}$.

This retardation mechanism may be understood through the craze stress redistribution. Fig. 9 shows the craze contour at the peak level of overload, compared with those before and after that load. The overload clearly widened the craze geometry in both thickness and length. After the overload cycle, the craze contour did not return to its previous geometry even at the same load.

The change of geometry is associated with the alteration of craze stress as shown in Fig. 10. In the overload cycle, the craze stress increases above the previous level over the entire length. Sometimes a small peak appears somewhere along the craze corresponding to the craze growth. After the overload cycle, however, the craze stress reduces over the most part of the craze, and the decrement near the crack tip is particularly dominant. Consequently, the craze stress decrement near the crack tip would depress fibril breakage there and hence result in crack growth retardation. The decreased craze stress at the crack tip may be related to the delayed duration. Fig. 11 indicates that the lower the attained peak stress is, the longer the retardation lasts.

After the overload application, contradictorily, the craze thickens more with smaller craze stress compared with the previous deformation. This may be explained by saying that the craze thickening during the overload period was brought about by new fibrillation from the craze-bulk boundary. In Fig. 12, the original craze thicknesses $g(r)$ before and after the

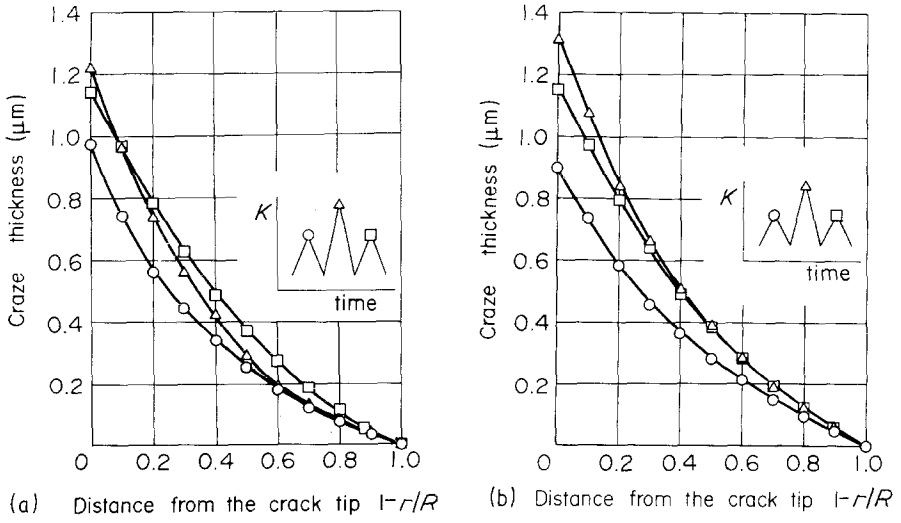

Figure 9 Craze contours before and after the overload (a) K_{IOL} = 0.85 MPa m$^{1/2}$, (b) K_{IOL} = 0.93 MPa m$^{1/2}$. (a) ○ K_I = 0.64 MPa m$^{1/2}$, R = 34 μm; △ K_I = 0.85 MPa m$^{1/2}$, R = 34 μm; □ K_I = 0.64 MPa m$^{1/2}$, R = 35 μm. (b) ○ K_I = 0.69 MPa m$^{1/2}$, R = 29 μm; △ K_I = 0.93 MPa m$^{1/2}$, R = 31 μm; □ K_I = 0.67 MPa m$^{1/2}$, R = 31 μm.)

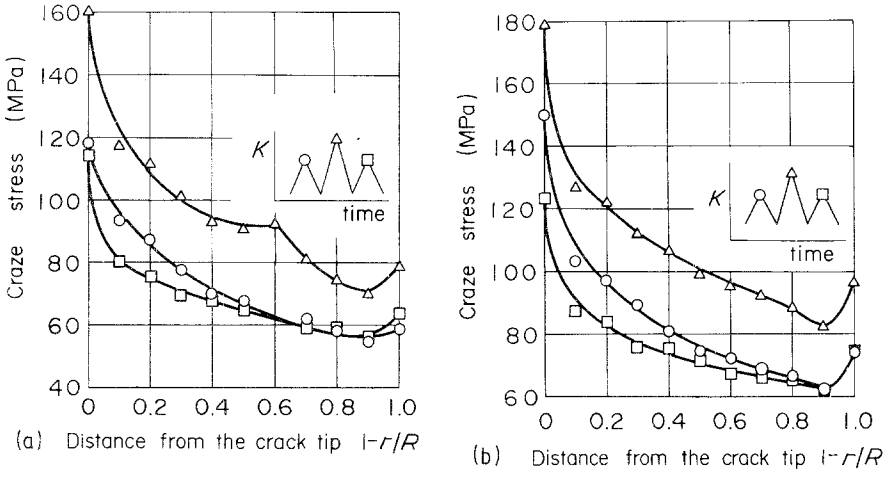

Figure 10 Craze stresses before and after the overload (a) K_{IOL} = 0.85 MPa $m^{1/2}$, (b) K_{IOL} = 0.93 MPa $m^{1/2}$ (symbols as Fig. 9).

overload are compared. The overload clearly increases the original thickness.

3.3. Stress–strain relation of craze fibrils

In the present calculation, the elastic modulus of matured craze fibril, F, was assumed to be 100 MPa. The ratio to Young's modulus of the bulk, F/E, was 0.03, which is a little higher than the value suggested by Döll *et al.* [7], 0.01 to 0.02. For PC, on the other hand, F/E = 0.15 was measured [10].

In order to look over the influence of craze modulus to the stress distribution, the calculation was executed for three different modulus values, 50, 100 and 300 MPa. The calculated stress distributions are shown in Fig. 13. Quite similar distributions were obtained except very near the crack tip. The reason may be as follows: to cancel the stress singularity at the craze tip, almost the same stress distribution is required no matter how much the craze modulus is.

The next question is, then, what the effect of the modulus is. Even for the same stress, crazes deform differently with moduli. In Fig. 14, the calculated original craze thickness $g(r)$ at the middle of the craze length was plotted for three different modulus values. For F = 50 and 300 MPa, the thickness $g(r)$ must decrease in the loading or unloading period in order to adjust the deformations between the surrounding bulk material and craze fibrils. The decrease of $g(r)$ means the craze fibril shrinkage into bulks. However, it may be unrealistic because the craze fibrillation is thought to be irreversible under ordinary testing conditions.

Consequently, it is preferable for $g(r)$ to increase at all times or at least remain almost constant during both loading and unloading like the case for F = 100 MPa, which may be the most suitable for this case.

As seen in Fig. 13, extremely high stresses are calculated near the crack tip. Since the fibril breakage occurs there resulting in the crack growth, an increase of stress is to be expected at that location. In the present calculation, however, another reason must be pointed out. The craze modulus F was assumed constant even at the crack tip up to fibril breakage. Crazes probably exhibit a non-linear stress–strain relation just before breakage, which would reduce the stress at the crack tip.

4. Conclusions

With reference to the previously proposed craze model, the numerical method of analysing the craze deformation has been demonstrated. This method takes the whole consistency between the refractive index, craze strain and craze boundary deformation and gives more detailed variations of craze stress and original craze thickness along the craze than before.

The craze stress concentrates at the crack tip with the applied load to result in fibril breakage. When the overload is applied in the course of fatigue cycling, the craze grows wider and sometimes longer accompanied

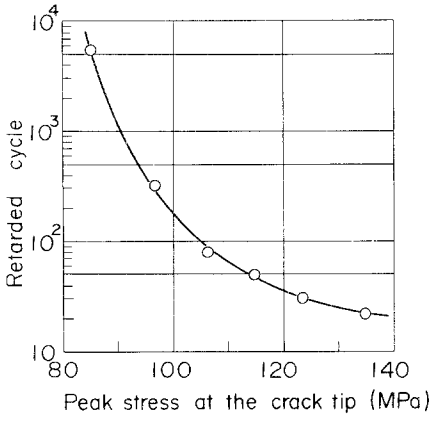

Figure 11 Retarded duration related to the peak stress attained at the crack tip after the overload.

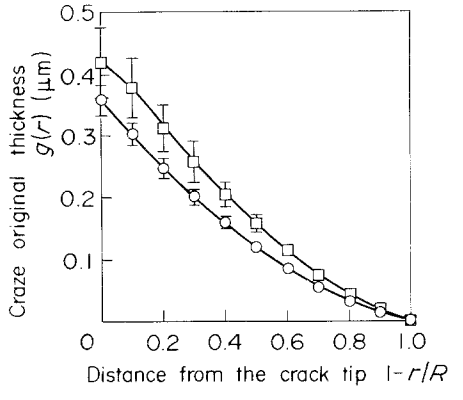

Figure 12 Craze original thicknesses before (○) and after (□) the overload. Mean values and the standard deviations in a complete one cycle are plotted. (K_I = 0.09 to 0.64 MPa $m^{1/2}$, K_{IOL} = 0.85 MPa $m^{1/2}$).

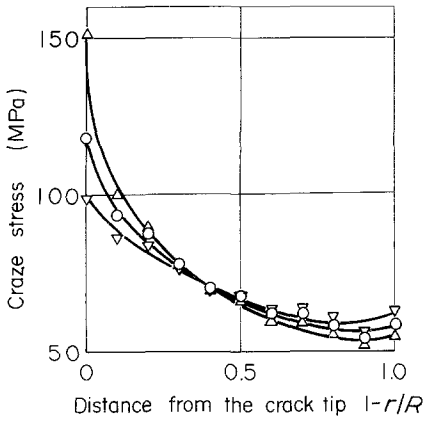

Figure 13 Effect of the craze modulus to the craze stress distribution (K_I = 0.64 MPa m$^{1/2}$, R = 34 μm, △ F = 300 MPa, ○ F = 100 MPa, ▽ F = 50 MPa).

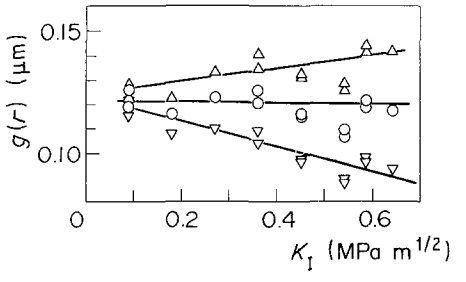

Figure 14 Trial calculation of the original craze thickness $g(r)$ at the middle of the craze length for three different moduli. (r/R = 0.50, △ F = 300 MPa, ○ F = 100 MPa, ▽ F = 50 MPa).

by an increase in the original thickness. Consequently, the crack tip stress reduces. It may be concluded, therefore, that this stress reduction is the cause of crack growth retardation after the overload.

References

1. A. C. KNIGHT, *J. Polym. Sci. A* **3** (1965) 1845.
2. E. J. KRAMER, in "Developments in Polymer Fracture 1", edited by E. H. Andrews (Applied Science Publications, London, 1979), Chapt. 3.
3. J. G. WILLIAMS, *J. Mater. Sci.* **12** (1977) 2525.
4. W. DÖLL, L. KÖNCZÖL and M. G. SCHINKER, *Polymer* **24** (1983) 1213.
5. B. D. LAUTERWASSER and E. J. KRAMER, *Phil. Mag.* **A38** (1979) 469.
6. H. R. BROWN and I. M. WARD, *Polymer* **14** (1973) 469.
7. W. DÖLL, in "Crazing in Polymers, Advances in Polymer Science 52/53", edited by H. H. Kausch (Springer-Verlag, Berlin, 1983) p. 105.
8. Y. IMAI and I. M. WARD, *J. Mater. Sci.* **20** (1985) 3842.
9. Y. W. MAI, *Int. J. Fracture* **15** (1979) R103.
10. R. P. KAMBOUR and R. W. KOPP, in Technical Information Series No. 67-C-374 (General Electric Company, Schenectady, USA, 1967).
11. T. CHAN, A. M. DONALD and E. J. KRAMER, *J. Mater. Sci.* **16** (1981) 676.
12. L. BEVAN, W. DOEL, L. KOENCZOEL, *J. Polym. Sci., Polym. Phys. Edn.* **24** (1986) 2433.

Received 23 May
and accepted 12 September 1988